
HOUSEHOLD SIZE CAN EXPLAIN 40% OF THE VARIANCE IN CUMULATIVE COVID-19 INCIDENCE ACROSS EUROPE

Seba Contreras^{1,2†*}, Philipp Dönges^{1,2†}, Maciej Filinski^{3†}, Joel Wagner^{1,2†}, Viktor Bezborodov³, Marcin Bodych³, Barbara Pabjan⁴, Franciszek Rakowski⁵, Jan Pablo Burgard^{6‡}, Tyll Krueger^{3‡*}, and Viola Priesemann^{1,2‡*}

¹Max Planck Institute for Dynamics and Self-Organization, Göttingen, Germany.

²Institute for the Dynamics of Complex Systems, University of Göttingen, Göttingen, Germany.

³Wroclaw University of Science and Technology, Poland.

⁴Institute of Sociology, University of Wroclaw, Poland.

⁵Interdisciplinary Centre for Mathematical and Computational Modelling, University of Warsaw, Poland.

⁶Trier University, Germany.

* Corresponding Authors: Seba Contreras (seba.contreras@ds.mpg.de), Tyll Krüger (tyll.krueger@pwr.edu.pl), Viola Priesemann (viola.priesemann@ds.mpg.de)

†, ‡ These authors contributed equally

Abstract

Household size impacts the spread of respiratory infectious diseases: Larger households tend to boost transmission by acquiring external infections more frequently and subsequently transmitting them back into the community. Furthermore, mandatory interventions primarily modulate contagion between households rather than within them. We developed an approach to quantify the role of household size in epidemics by separating within-household from out-household transmission, and found that household size explains 41% of the variability in cumulative COVID-19 incidence across 34 European countries (95% confidence interval: [15%, 46%]). The contribution of households to the overall dynamics can be quantified by a boost factor that increases with the effective household size, implying that countries with larger households require more stringent interventions to achieve the same levels of containment. This suggests that households constitute a structural (dis-)advantage that must be considered when designing and evaluating mitigation strategies.

Introduction

Emerging and re-emerging respiratory infectious diseases, exemplified by the recent COVID-19 pandemic, highlight the urgent need for robust pandemic preparedness plans. This requires identifying the factors that determine how a disease spreads within the population, thereby providing a basis for the informed design of public health interventions, such as non-pharmaceutical interventions (NPIs). However, these measures typically target community transmission and have little effect in controlling transmission within households [1–3]. In addition, household contacts differ from external interactions: they are prolonged and more proximal, thereby increasing the likelihood of transmission. Once a pathogen enters a household, the probability of spreading to other members is high, making households potent accelerators of disease transmission [4–6]. Therefore, to implement effective NPIs, it is critical to understand how household structure (i.e., household size distribution) impacts epidemics [5, 7–13].

Across countries, incidence, prevalence, and excess mortality varied widely, also for the COVID-19 pandemic. Across Europe, this variation cannot exclusively be attributed to differences in how NPIs were implemented [14–17]. While differences in demographics [18], culture [19, 20], trust in the government [21], and resources [22] can explain some of the variation, all these factors covary with a country's most fine-grained functional unit: household structures. It thus remains open to determine how much of the observed variation in prevalence can be explained by household size alone.

To address this question, we first developed a mathematical framework to distinguish between within- and out-household disease spread. Broadly speaking, within-household contacts "boost" the spread of the disease, whereas out-household contacts modulate the overall reach of an outbreak. We then quantified the out-household spread for 34 European countries, allowing us to rank them according to their mitigation of out-household spread. Noting that households are also part of major socioeconomic indicators correlated with the observed prevalence, such as the Human Development Index (HDI), we finally quantified the extent to which household size contributes to this correlation by computing the semi-partial correlation, controlling for household effects. These combined analyses demonstrate that nations with larger households faced an inherent disadvantage in mitigating the impacts of the COVID-19 pandemic. This is because the larger the structural boost induced by households, the lower the effective out-household spread allowed for containment.

Results

Separating out- from within-household transmission

By separating out- from within-household disease spread, we can quantify how much of the transmission can be modified by NPIs. Focusing on the out-household contacts first, we can study disease spread in a network of households where partially infectious households infect others through bridges of mutual contact (Fig. 1A). We can then define a *household reproduction number* \mathcal{R}_H as the spread between households, i.e., the expected number of households that are infected by one infectious household during the outbreak. As derived in Section S1, \mathcal{R}_H can be written as the product of the out-household spread and a household-dependent "boost" factor

$$\mathcal{R}_H = R_{\text{out},t} \mathcal{B}. \quad (1)$$

$R_{\text{out},t}$ is the average out-household reproduction number at a given time t , defined as the expected number of individuals that a typical individual infects *outside* of their household, assuming that all contacts are susceptible. As $R_{\text{out},t}$ does not include immunity or its loss, it can be understood as a basic reproduction number, adjusted to exclude within-household contagion. Knowing the household size distribution η of the country (i.e., the probability $P(k)$ that a randomly selected household consists of k members) and the in-household secondary attack rate of the disease a_H —which quantifies the expected fraction of the household that is infected in an outbreak—the household "boost" \mathcal{B} to the spreading dynamics can be derived as

$$\mathcal{B} = 1 + a_H (\eta^* - 1), \quad (2)$$

where η^* is the effective household size, defined as the ratio between the second and first statistical moments of η , mathematically equivalent to the mean of η plus a variance-dependent correction factor (see Methods S1 for details). Intuitively, we subtract one from η^* in (2), because the person who brings the infection into the household cannot be infected again. Note that \mathcal{B} solely depends on η^* , not on the full household size distribution η .

The critical value $\mathcal{R}_H = 1$ delimits the transition between subcritical and supercritical disease spread. Consequently, the critical out-household reproduction number is inverse to the household boost factor, $R_{\text{out}}^{\text{crit}} = \mathcal{B}^{-1}$, and thus depends on the effective household size η^* (Fig. S8). The implications of this relationship are far-reaching: countries or regions with larger effective household size η^* reach critical disease spread at smaller values of $R_{\text{out}}^{\text{crit}}$, and thus require stronger interventions to mitigate an outbreak than countries with smaller η^* (see Fig. 1B for an overview of effective household size across Europe). With η^* varying between 2.6 and 4.2 across Europe, and assuming a within-household secondary attack rate of $a_H = 0.2$, the critical reproduction number $R_{\text{out}}^{\text{crit}}$ differs between 0.75 and 0.61, respectively.

To calculate the \bar{R}_{out} , defined as the average ρ_i over all infectious individuals in an outbreak I , we need to know the prevalence α , which coincides with the cumulative incidence when re-infections are not common (in the time window considered). We proceeded as described in Fig. 1C: we used age-specific infection fatality rates (IFRs) and country demographics to estimate country-specific infection fatality rates (CIFRs). With these CIFRs, we estimated COVID-19 deaths, including a fraction of the surplus deaths (similar to [17]), and COVID-19 prevalence α for the time period from January 1st, 2020 (before COVID-19 cases or deaths were reported in Europe), until June 13th, 2021. This end date was selected because it marks a period when

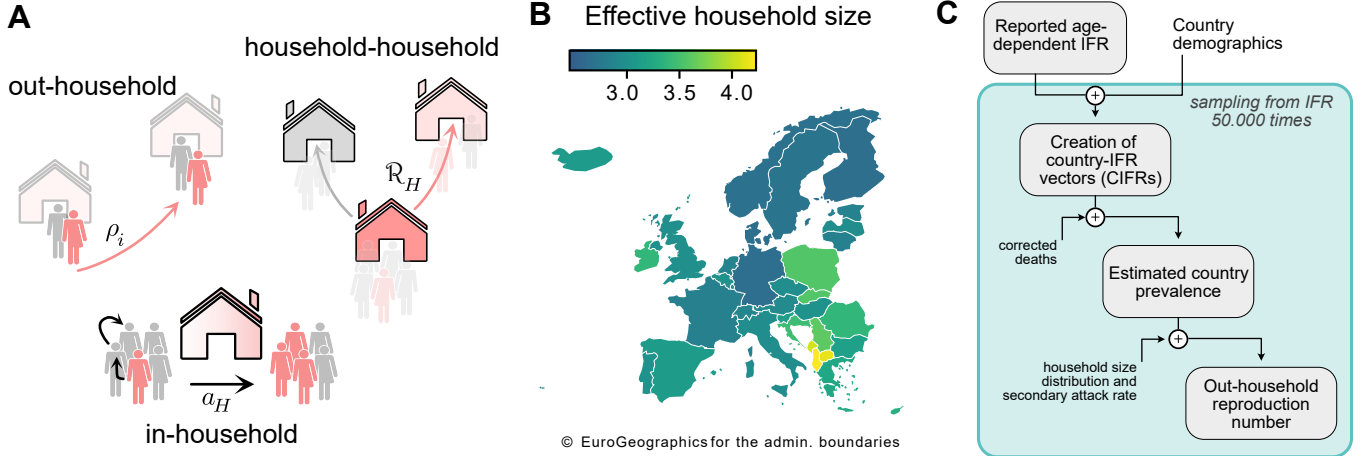


Figure 1: Disease spread from the perspective of households. **A.** Disease spread can be categorized into the contagion occurring outside and inside of households. ρ_i quantifies the number of potentially contagious contacts of an individual i . The out-household reproduction number \bar{R}_{out} is defined as the mean ρ_i , averaged over all infectious individuals in an outbreak I . Once an infectious individual enters a household of size k , the in-household secondary attack rate a_H quantifies the in-household outbreak as the fraction of the $k - 1$ members who are infected. The household reproduction number \mathcal{R}_H is defined as the expected number of households a typical infectious household infects. **B.** Variation of the effective household size η^* across European countries. **C.** Methods overview: Using age-dependent infection fatality rates (IFRs) and country demographics, we obtained country-specific IFR samples (CIFRs). Combined with an estimate for the number of COVID-19 deaths, we estimated the COVID-19 prevalence (cumulative incidence) for each country. Finally, combining country-specific prevalences, household size distributions, and in-household secondary attack rates, we computed the out-household reproduction number \bar{R}_{out} .

infection numbers were consistently low across all considered countries [23], which is required for accurately averaging \bar{R}_{out} over an entire wave. Combined with the household size distribution η [24], we calculate \bar{R}_{out} . To propagate the uncertainty in the IFR estimation, we sampled from the distributions reported in [25, 26] and repeated the process 50 000 times, obtaining distributions of prevalences and \bar{R}_{out} . Details and robustness checks are provided in the Supplementary Material, Sections S1 and S3 respectively.

Effective household size as a structural (dis-)advantage for pandemic control

We derived the impact of household size on COVID-19 spread, and thus on the prevalence α , by assuming (counterfactually) that all European countries had the same out-household reproduction number $\bar{R}_{\text{out,Europe}}$. As described in the Methods section, this assumption enabled us to quantify the impact of the effective household size on α (gray crosses, Fig. 2A). Differences between the expected (gray) and observed (colored) prevalence account for variations in local epidemic management, specifically the effectiveness of mitigation measures. Thus, they indicate how well the disease was mitigated in a given country, factoring out the contribution of households. Countries below the theoretical curve achieved a higher reduction in out-household contagion compared to those above it (residuals in Fig. 2B). Note that this apparent success may reflect effective interventions but also differences in other factors, such as culture, compliance, resources, and weather.

As predicted from Eq. (1), the theoretical prevalence increases with the effective household size η^* . Furthermore, there is a clear correlation between the effective household size η^* and the observed prevalence α (Pearson's

correlation 0.69 (95% CI: [0.63, 0.75]), p-value 4.16×10^{-6} (95% CI: $[2.78 \times 10^{-7}, 4.76 \times 10^{-5}]$) Fig. 2C). Quantitatively, η^* explains 40.6% (95% CI: [14.7%, 46.1%]) of the variance in the data (Fig. 2D).

Comparison of out-household contagion across European countries

Quantifying out-household disease spread via \bar{R}_{out} offers a way to assess the effectiveness of NPIs in each country, factoring out the contribution of households to the overall dynamics. Using the observed prevalence for each country, we obtained country-specific distributions for \bar{R}_{out} (Fig. 3A) and its deviation from the European mean (Fig. 3B), and sorted the countries in order of increasing median. This sorting induces a ranking for the (out-household) effectiveness of NPIs. As the positions in the ranking may vary for different sets of CIFR vectors, we obtained a distribution over the ranking positions for each country (Fig. 3C). As in Fig. 2, the same groups of countries fall into similar ranges (Fig. 3), with countries of Central and Eastern Europe displaying higher values of \bar{R}_{out} and thus ranking lower than the Nordic and island countries. It is thus necessary to understand the cultural and sociological processes behind the household structure and size that may induce such clustering.

The structure and size of households result from long-term economic and cultural processes, hence their variation across countries. For example, in 2020, there were more single-adult households without children

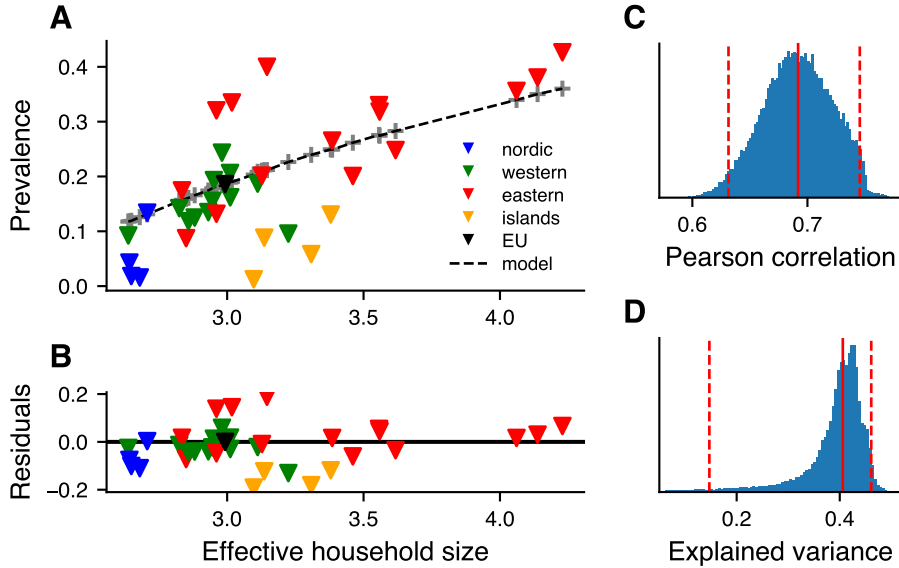


Figure 2: Differences in the effective household size can explain about 40% of the variation in COVID-19 prevalence across European countries in the first pandemic year. **A.** We analyzed a hypothetical scenario where all European countries had the same out-household spread (computed by treating Europe as a single country), namely, the same conditions (NPIs, climate, social culture) except for their household size distribution. By doing so, we calculated theoretical prevalences (gray crosses and black dashed line) and interpreted deviations from them as differences in the effective reduction of out-household contagion across countries (**B**). Besides the strong correlation between observed prevalence and effective household size (**C**), the latter explains 40.6% (95% CI: [14.7%, 46.1%]) of the variance observed in the former (**D**). Countries are color-coded as follows: Nordic countries (blue), Western European countries (green), and post-communist countries of Central and Eastern Europe (red), and island countries (yellow). Note that, following the method in Fig. 1C, the result is a distribution of theoretical prevalence, which is not shown in this figure for clarity. A larger version with country labels is available in the Supplementary Section S7.

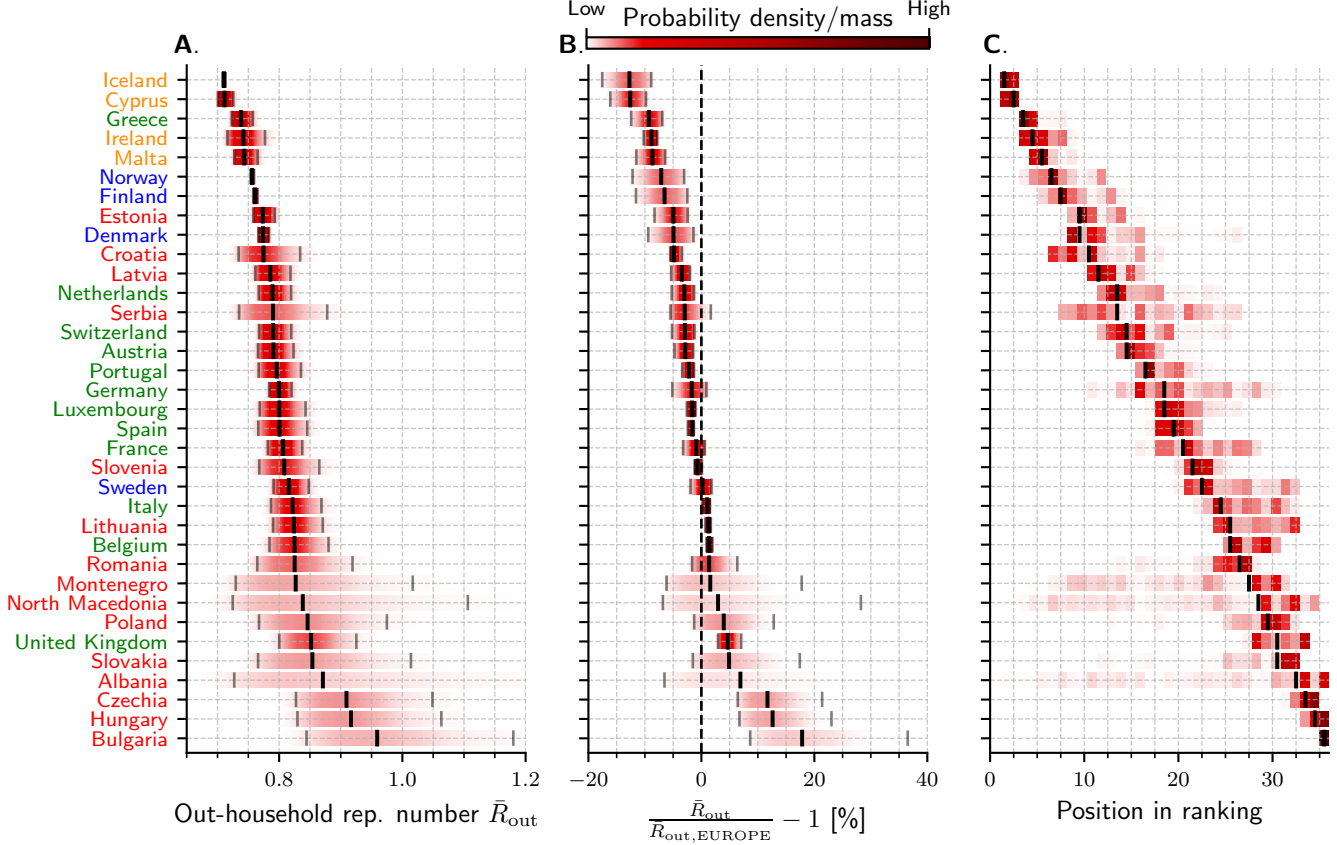


Figure 3: **Out-household COVID-19 spread across European countries.** **A, B.** Using our prevalence estimations and country-specific infection fatality rates (CIFR), we computed the \bar{R}_{out} distributions (**A**) and their deviations from the European mean (**B**) (countries ranked in order of increasing median) for the timeframe between January 1st, 2020, and June 13th, 2021. **C.** As positions in the ranking for different CIFR vectors are correlated, we obtained a distribution over the possible ranking spots for each country. Vertical lines represent the median and 95% CIs, and color bars represent the probability density or mass.

and single-parent households with children in Nordic countries than in Central and Eastern Europe [27]. Furthermore, a higher share of extended family households was found in central-eastern Europe, particularly in Bulgaria (17.3%), Poland (11.1%), Latvia (11.1%), and Romania (10.3%), whereas in Nordic countries, extended households constitute less than 1% [28,29]. As shown in Fig. 3A, the pattern of \bar{R}_{out} across countries appears to align with differences in income, with lower-income countries generally experiencing higher \bar{R}_{out} . In contrast, Scandinavian and Western European countries show the opposite trend. An exception lies in Island states; Greece and Cyprus, which have low incomes, managed to maintain relatively low \bar{R}_{out} . During the COVID-19 pandemic, Socio-geo-economic factors have been linked to the levels of morbidity and mortality [30,31], and we show that the effectiveness of interventions in reducing out-household spread also seems to follow these patterns.

Human development index, household size, and COVID-19 prevalence

As seen in the previous sections, households have a pronounced impact on COVID-19 prevalence. However, they are also a structural part of major socioeconomic indicators, such as the Human Development Index

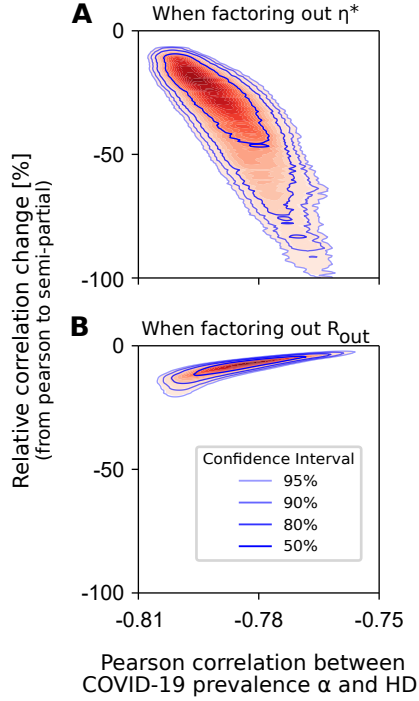


Figure 4: **Effective household size η^* and the out-household rep. number \bar{R}_{out} influence the correlation between COVID-19 prevalence α and the Human Development Index (HDI).** We used the semi-partial correlation to quantify the relative change in the correlation (Pearson vs. semi-partial) between α and HDI when removing the influence of η^* (A) and \bar{R}_{out} (B) from α .

(HDI), that are strongly correlated with the observed prevalence α (median Pearson correlation coefficient between COVID-19 prevalence and HDI: $r = -0.79$, median p-value $p = 2.15 \times 10^{-8}$ Fig. 4). Here, using the method of semi-partial correlation, we show that the effective household size explains a substantial portion of the correlation observed between COVID-19 prevalence and HDI. The semi-partial correlation is particularly useful for this purpose, as it quantifies how much of the correlation remains between the residuals of a regression curve (a linear model when another approach is not available) and another variable.

The semi-partial correlation between α and the HDI after accounting for the effective household size is lower than the Pearson correlation (median $r = -0.52$, $p = 0.0015$, Fig. 4), implying that a large portion of the correlation between prevalence and HDI can be attributed to the influence of the household distribution (median reduction of 34.4% (95% CI: [11.1%, 94.3%]) Fig. 4A). In contrast, its value when factoring out the out-household reproduction number (median $r = -0.72$, $p = 1.09 \cdot 10^{-6}$) does not deviate as much from the original Pearson correlation, accounting for a weaker contribution (median reduction of 8.5% (95% CI: [3.6%, 18.6%]) Fig. 4B). All values and confidence intervals are available in Table S2. This example illustrates the importance of controlling for households in correlation models and how our theory enables us to do so.

Discussion

Because household contacts are closer than most other social interactions, it is intuitive that they may have a substantial impact on how epidemics unfold. This work presents a conceptual and theoretical framework for

quantifying the extent of this effect and provides evidence for the impact of the household size distribution on COVID-19 spread.

Our framework enables us to isolate the contribution of households to disease spread, rewriting the epidemic threshold as the product of a household-boost factor \mathcal{B} and a critical out-household reproduction number $R_{\text{out}}^{\text{crit}}$. The boost factor increases linearly with the effective household size η^* , in line with the results of previous theories [8, 9, 12]. This means that countries with larger households face a structural disadvantage and need stronger contact reduction between households to achieve the same containment levels. The out-household reproduction number \bar{R}_{out} factors out the contribution of households while encompassing all factors contributing to out-household disease spread, including culture, weather, overall compliance with interventions, and their effectiveness, making it a comprehensive index. We therefore propose using \bar{R}_{out} as a new index to measure and compare out-household contagion across countries or regions.

On the evidence side, we showed that households explain 40.6% (95% CI: [14.7%, 46.1%]) of the variance in COVID-19 incidence across 34 European countries. In fact, the correlation between the effective household size and the observed prevalence is strong (Pearson's correlation 0.69 (95% CI: [0.63, 0.75]) and statistically significant (median p-value 4.2×10^{-6}). We identified distinct groups of countries whose observed prevalence deviates from the reference curve, forming separate clusters. Deviations from this curve provide a measure of pandemic mitigation across countries, factoring out the contribution of households.

We extensively reviewed the literature to obtain accurate parameter values for our model. Regarding the in-household secondary attack rate a_H , although increasing, the overall value across 81 studies published until June 2021 was 18.1% (95% CI: [15.4%–21.3%]) [32, 33], and showed a weak dependence on household size. Additionally, our framework can be easily extended to incorporate vaccination, age groups, and other structural levels in contact patterns (e.g., workplaces), which may be relevant for secondary transmission [34].

Our approach to estimating the country-specific COVID-19 prevalence used an estimate of COVID-19-related deaths, as seroprevalence studies at the population scale and across all regions we analyzed were unavailable, e.g., in [35]. There are several studies dedicated to the estimation of worldwide COVID-19-related deaths, e.g., [17, 36]; however, there are strong discrepancies from what local teams have reported (see, e.g., [37–40]). We conducted a comprehensive analysis and parameter scanning in the Supplementary Materials to confirm that our results remain valid within the reported parameter and variable ranges. We also tested and verified the reliability of our results using alternative methodologies and provided original data to support our parameter choices.

To sum up, household structure, a cornerstone of cultural diversity worldwide, is a resilient entity that endures despite the influence of contemporary economic and political factors. Understanding the structural challenges that countries and regions face due to their household structures and their potential to accelerate epidemics is an urgent need in our efforts to enhance preparedness and effectively respond to future threats to global public health.

Methods

The relation between prevalence, household structure, and out-household reproduction number

We consider a network SIR (susceptible-infectious-recovered) epidemic framework with households and possible time-varying out-household contact structures. Each infected individual in the network has an

unknown out-household reproduction number ρ_i at the time the individual became infected, where i indexes the cumulative set of infected individuals at time t , I (for ease of notation, we will ignore the explicit time dependence). The term *infected* involves the currently infectious and the recovered (assumed to be immune). We also assume a household-size-independent in-household secondary attack rate a_H , although the theory remains valid for household-size-dependent attack rates.

Let the population be denoted by n ($n \gg 1$), H_k the number of households of size k , and $H = \sum H_k$ the total number of households. The household size distribution η is thus defined as $\eta_k = \frac{H_k}{H}$. Let further $E(\eta) = \sum_k k\eta_k$ be the average household size. It follows that $\sum_k kH_k = n = H \cdot E$ and hence $H = \frac{n}{E}$. First, we compute the probability that an individual had an infectious out-household contact, p_{out} . Note that having an infectious out-household contact does not mean the individual was infected by that contact, as they may already have been infected earlier by an infectious in-household contact. Let α denote the prevalence in the population, which, under the assumption of perfect immunity after infection, can be expressed as $\alpha \stackrel{\text{def}}{=} \frac{I}{n}$. For $n \rightarrow \infty$ we obtain the probability for an infectious out-household contact p_{out} as

$$p_{\text{out}} = 1 - \prod_{i \in I} \left(1 - \frac{\rho_i}{n}\right) \quad (3)$$

$$\simeq 1 - \exp\left(-\frac{1}{n} \sum \rho_i\right) \quad (4)$$

$$= 1 - \exp\left(-\frac{\alpha}{I} \sum \rho_i\right) \quad (5)$$

$$= 1 - \exp(-\alpha \cdot \bar{R}_{\text{out}}), \quad (6)$$

where $\bar{R}_{\text{out}} = \frac{\sum_{i \in I} \rho_i}{I}$ is the average of the individual ρ_i .

In the following, we show how the out-household infection probability p_{out} and the household secondary attack rate a_H (more generally, the assumptions on the in-household transmission probabilities) determine the expected number of infected household members. Let $\mu_k = \mu_k(p_{\text{out}})$ represent the expected number of infected individuals in a household of size k . Furthermore, η_k and μ_k are directly related to the prevalence α , enabling the computation of the out-household reproduction number \bar{R}_{out} , given a_H . We have,

$$\sum_{k \geq 1} H_k \mu_k = \alpha \cdot n \quad (7)$$

$$\text{and hence} \quad (8)$$

$$\sum_{k \geq 1} \eta_k \mu_k = E \cdot \alpha. \quad (9)$$

For $\mu_k(p_{\text{out}})$ we have

$$\mu_k(p_{\text{out}}) = \sum_{l=1}^k d_{l,k} \binom{k}{l} p_{\text{out}}^l (1 - p_{\text{out}})^{k-l}, \quad (10)$$

where $d_{l,k}$ is the expected number of infected individuals in a household of size k if $l \geq 1$ household members were exposed to infection from outside the household. In general, $d_{l,k}$ can be expressed via recursions. In the following, we illustrate a possible way to compute $d_{l,k}$ when the in-household infection process is described

via an Erdős-Rényi random graph model with edges representing infections with edge probability $p_k = p(k)$ (which might be different for different household sizes k). To compute $d_{l,k}$, we have to estimate the probability that exactly m nodes are connected to at least one of the fixed l externally exposed household members. Let $P_l(m, k)$ be this probability. Let further $Q_l(k, p_k)$ be the probability that in a household of size k with l external exposures, all household members will become infected. As a natural consequence, $Q_l(l, p_k) = 1$ always holds. We have

$$Q_l(k, p_k) = 1 - \sum_{m=l}^{k-1} \binom{k-l}{m-l} Q_l(m, p_k) (1-p_k)^{m(k-m)} \quad (11)$$

and

$$P_l(m, k) = \binom{k-l}{m-l} Q_l(m, p_k) (1-p_k)^{m(k-m)}. \quad (12)$$

Finally, we get

$$d_{l,k} = \sum_{m=l}^k m P_l(m, k). \quad (13)$$

To start the recursion, one starts with $Q_l(l, p_k) = 1$ and proceeds by iteratively computing $Q_l(l+i, p_k)$ for $i = 1, 2, \dots$ (up to households of size 6, as the Eurostat household size distributions are truncated at that value [24]) using Eq. 11. With the $Q_l(l, p_k)$ one proceeds to compute the $P_l(m, k)$ and $d_{l,k}$. With the $d_{l,k}$ one can compute the $\mu_k(p_{\text{out}})$, via which one solves $\sum_{k \geq 1} \eta_k \mu_k = E \cdot \alpha$ for p_{out} . Via Eq. 6, this offers a relation

between the prevalence α , the household size distribution η , and the out-household reproduction number \bar{R}_{out} .

Lastly, to estimate the values of p_k for different household sizes, we choose a fixed in-household secondary attack rate $a_H = 0.2$ (assumed to be independent of the household size k), defined as the expected number of secondary cases generated from a first, single infection of the household from outside. Hence, we solve the above recursion equations for $d_{l,k}$ such that $a_H = (d_{1,k} - 1) / (k - 1)$ is equal to a constant a_H . Once the $d_{l,k}$ have been computed as a function of the p_k , one can solve the fixed point equation $\sum_{k \geq 1} \eta_k \mu_k = E \cdot \alpha$, which has a nontrivial solution for p_{out} and hence for \bar{R}_{out} (Eq. 6) when the household reproduction number (defined in the next section, Eq. 17) is $\mathcal{R}_H > 1$.

Table 1: **Model variables.**

Variable	Name	Formula
ρ_i	Individual out-household reproduction number	–
\bar{R}_{out}	Average out-household reproduction number	$\bar{R}_{\text{out}} = \frac{1}{I} \sum \rho_i$
η^*	Effective household size	$E(\eta) + \frac{\text{Var}(\eta)}{E(\eta)}$
α	Prevalence	–
\mathcal{B}	Household boost factor	$\mathcal{B} = 1 + a_H (\eta^* - 1)$
\mathcal{R}_H	Household reproduction number	$\mathcal{R}_H = R_{\text{out},t} \mathcal{B}$

Table 2: **Model parameters.**

Parameter	Name	Value (default, range)	Source
a_H	In-household secondary attack rate	0.2 [0.18 – 0.22]	[32, 34]
γ	Fraction of excess deaths attributable to COVID-19	0.85 [0.70 – 1.00]	Estimated
η	Household size distribution	country specific	[24]

The household reproduction number \mathcal{R}_H

Here, we describe the initial infection process between households and derive the equation for the household reproduction number. The phase transition for the emergence of a giant component in random graphs with household structures and its relation to epidemics has already been studied in great detail in the works of F. Ball (see, e.g., [41]). Here, we give a short derivation of the equation for the household reproduction number based on the theory of inhomogeneous random graphs. We consider a directed random graph model where edges stand for potential infectious contacts, where the probability that an infected individual i will infect an individual j is given by

$$\Pr(i \rightsquigarrow j) = \frac{\rho_i}{n}. \quad (14)$$

We assume that edges are independent, the values ρ_i are independent of the household size, and the ρ_i distribution has an asymptotic limiting distribution for large n with finite expectation $R_{\text{out},t}$. The network defined by this edge formation rule would be a directed Bollobas-Janson-Riordan graph [42], also known as an inhomogeneous random graph, if some mild conditions on the ρ_i distribution were imposed, e.g., boundedness or a finite first moment. Additionally, the population is partitioned into households. Hence, the out-household network structure induces a network structure among the households. We can describe the household connectivity structure using a kernel that specifies the probability that an infected household of size x is connected to a household of size y (note that all edges represent infectious events). It is given by the household contact kernel \varkappa_H :

$$\Pr(x \rightsquigarrow y) = \frac{\varkappa_H(x, y)}{H} \quad (15)$$

$$\varkappa_H(x, y) = \frac{R_{\text{out},t}}{E(\eta)} (1 + a_h(x - 1)) \cdot y, \quad (16)$$

The connectivity properties of the network of households determine the epidemic threshold. The threshold criterion can be formulated as the condition that the household-reproduction number \mathcal{R}_H (defined as the average number of secondary households infected by an infected household) equals one. Applying the general theory for directed Bollobas-Janson-Riordan graphs [43] (see also the appendix in [3]), we obtain the household reproduction number

$$\mathcal{R}_H = R_{\text{out},t} (1 + a_H(\eta^* - 1)), \quad (17)$$

where the effective household size η^* emerges as the quotient between the second and first statistical moments of η .

We close this section by providing a relation between the out-household reproduction number $R_{\text{out},t}$ at a given time and the average out-household reproduction number \bar{R}_{out} , averaged over all infected individuals in an outbreak. Recall that $R_{\text{out},t}$ is the mean number of secondary cases generated by newly infected individuals at time t (here, we consider t to be a discrete-time unit, e.g., a day or a week, short enough that changes of $R_{\text{out},t}$ within such a time unit can be neglected). Let furthermore I_t be the newly infected individuals at time t . We then have the relation

$$\bar{R}_{\text{out}} = \sum_{t=0}^T R_{\text{out},t} \cdot I_t / \sum_{t=0}^T I_t. \quad (18)$$

Partial correlation analysis

The estimated prevalence α correlates with socioeconomic indicators, such as the Human Development Index (HDI) and its components. However, both quantities are (directly or indirectly) affected by other variables, such as the effective household size η^* or the out-household reproduction number \bar{R}_{out} . We aim to quantify how much of the correlation between prevalence and the HDI remains after excluding the contributions of those variables. The semi-partial correlation quantifies how much of the correlation remains between two variables (HDI and prevalence α) when the influence of a third variable is removed from only one of them (η^* or \bar{R}_{out} from COVID-19 prevalence) [44]. In contrast, the partial correlation quantifies how much of the correlation remains after controlling for the variable that influences both variables. The following paragraph outlines how to compute both the partial and semi-partial correlations.

Generally, if the relationships among all variables are linear, the partial correlation can be computed as follows. Let $X = (x_1, \dots, x_N)$ and $Y = (y_1, \dots, y_N)$ be the correlating variables, and $Z = (z_1, \dots, z_N)$ be the confounding variable that influences both X and Y . First, one conducts two separate linear regressions with the confounding variable, namely one between X and Z and the other between Y and Z . Let e_X and e_Y be the residuals of the two linear regressions. The partial correlation $r_{XY,Z}$ is then given by the Pearson correlation coefficient between the residuals e_X and e_Y . As the residuals represent the relationship not accounted for by the confounding variable, this method excludes its contribution. In case the confounding variable only influences X , the semi-partial correlation can be computed as the Pearson correlation between the residuals e_X with the variable Y itself, i.e., without performing the linear regression between Y and Z .

In our case, the semi-partial correlation is computed as the Pearson correlation between the residuals e_α and the HDI. However, because our framework provides a nonlinear theoretical relationship between the prevalence α and the confounding variables, the residuals e_α are not computed via linear regression but rather using the theoretical prevalences as described in the main text. When the confounding variable is η^* , the theoretical prevalences are computed assuming a common \bar{R}_{out} across countries. Vice versa, when the confounding variable is \bar{R}_{out} , theoretical prevalences are computed under the assumption of a constant household distribution across countries. The residuals are then correlated with the HDI across all samples for each IFR vector, yielding a distribution of semi-partial correlation coefficients.

Data sources

Prevalence estimates are based on annual population size, weekly deaths from all causes, and reported COVID-19 deaths (for details, see SI, Section S1.1.2). The first two datasets, covering 2015–2021, come from Eurostat. However, they are incomplete for some countries; for instance, overall death data are missing for Ireland, Luxembourg, and North Macedonia. Without complete all-cause mortality data, excess deaths cannot be estimated. Nevertheless, prevalence for these countries can still be inferred from officially reported COVID-19 deaths. To this end, we used a dataset of daily reported COVID-19 deaths from Johns Hopkins University, which covers all European countries, and aggregated it to weekly counts.

Acknowledgements

We thank the Priesemann group for the exciting discussions and their valuable input. Authors with affiliation "1" received support from the Max-Planck-Society. SC, PD, VP, and TK were funded by the German Federal Ministry for Education and Research for the RESPINOW project (031L0298G), and SC, VP, and JW by the infoXpand project (031L0300A). VP was supported by the Deutsche Forschungsgemeinschaft (DFG, German Research Foundation) under Germany's Excellence Strategy - EXC 2067/1-390729940. VP also acknowledges the support of the Ministry of Science and Culture of Lower Saxony through funds from the program zukunft.niedersachsen of the Volkswagen Foundation for the 'CAIMed – Lower Saxony Center for Artificial Intelligence and Causal Methods in Medicine' project (grant no. ZN4257), "Niedersächsisches Vorab", and the Niedersachsen-Profil-Professur. TK acknowledges support from the Government of Saxony through the SaxoCOV grant. Grammarly Pro AI has been used for grammar checks.

Author Contributions

Conceptualization: JPB, TK, VP

Data curation: FR, JW, MF, PD

Formal analysis: JPB, JW, MF, PD, TK, VB

Funding acquisition: SC, TK, VP

Investigation: BP, FR, JPB, JW, MB, MF, PD, SC, VP

Methodology: FR, JPB, MB, PD, TK

Project administration: SC, TK, VP

Resources: TK, VP

Software: JPB, JW, MF, PD, JPB

Supervision: SC, TK, VP

Validation: all

Visualization: JW, MF, PD, SC

Writing - Original Draft: BP, FR, JPB, JW, MF, PD, SC, TK, VP

Writing - Review & Editing: all

References

- [1] Damilola Victoria Tomori, Nicole Rübsamen, Tom Berger, Stefan Scholz, Jasmin Walde, Ian Wittenberg, Berit Lange, Alexander Kuhlmann, Johannes Horn, Rafael Mikolajczyk, et al. Individual social contact data and population mobility data as early markers of sars-cov-2 transmission dynamics during the first wave in germany—an analysis based on the covimod study. *BMC medicine*, 19:1–13, 2021.
- [2] Kerry LM Wong, Amy Gimma, Pietro Coletti, Christel Faes, Philippe Beutels, Niel Hens, Veronika K Jaeger, Andre Karch, Helen Johnson, et al. Social contact patterns during the covid-19 pandemic in 21 european countries—evidence from a two-year study. *BMC infectious diseases*, 23(1):268, 2023.
- [3] Philipp Dönges, Thomas Götz, Nataliia Kruchinina, Tyll Krüger, Karol Niedzielewski, Viola Priesemann, and Moritz Schäfer. Sir model for households. *SIAM Journal on Applied Mathematics*, 84(4):1460–1481, 2024.

- [4] Michiel van Boven, Christiaan H van Dorp, Ilse Westerhof, Vincent Jaddoe, Valerie Heuvelman, Liesbeth Duijts, Elandri Fourie, Judith Sluiter-Post, Marlies A van Houten, Paul Badoux, et al. Estimation of introduction and transmission rates of sars-cov-2 in a prospective household study. *PLOS Computational Biology*, 20(1):e1011832, 2024.
- [5] Signe Møgelmose, Laurens Vijnck, Frank Neven, Karel Neels, Philippe Beutels, and Niel Hens. Population age and household structures shape transmission dynamics of emerging infectious diseases: a longitudinal microsimulation approach. *Journal of the Royal Society Interface*, 20(209):20230087, 2023.
- [6] Subekshya Bidari and Wan Yang. The impact of household size on measles transmission: A long-term perspective. *Epidemics*, 49:100791, 2024.
- [7] Joe Hilton and Matt J Keeling. Incorporating household structure and demography into models of endemic disease. *Journal of the Royal Society Interface*, 16(157):20190317, 2019.
- [8] Frank Ball, Denis Mollison, and Gianpaolo Scalia-Tomba. Epidemics with two levels of mixing. *The Annals of Applied Probability*, pages 46–89, 1997.
- [9] Frank G Ball and Owen D Lyne. Epidemics among a population of households. In *Mathematical Approaches for Emerging and Reemerging Infectious Diseases: Models, Methods, and Theory*, pages 115–142. Springer, 2002.
- [10] Thomas Götz. Modeling household effects in epidemics. In *Predicting Pandemics in a Globally Connected World, Volume 2: Toward a Multiscale, Multidisciplinary Framework through Modeling and Simulation*, pages 71–97. Springer, 2024.
- [11] Philipp Doenges, Thomas Götz, Tyll Krueger, Karol Niedzielewski, Viola Priesemann, and Moritz Schaefer. Sir-model for households. *arXiv preprint*, page 2301.04355, 2023.
- [12] Thomas House and Matt J Keeling. Deterministic epidemic models with explicit household structure. *Mathematical biosciences*, 213(1):29–39, 2008.
- [13] T House and Matthew James Keeling. Household structure and infectious disease transmission. *Epidemiology & Infection*, 137(5):654–661, 2009.
- [14] Ariel Karlinsky and Dmitry Kobak. Tracking excess mortality across countries during the covid-19 pandemic with the world mortality dataset. *Elife*, 10:e69336, 2021.
- [15] Mrinank Sharma, Sören Mindermann, Charlie Rogers-Smith, Gavin Leech, Benedict Snodin, Janvi Ahuja, Jonas B Sandbrink, Joshua Teperowski Monrad, George Altman, Gurpreet Dhaliwal, et al. Understanding the effectiveness of government interventions against the resurgence of covid-19 in europe. *Nature communications*, 12(1):5820, 2021.
- [16] Thomas Hale, Noam Angrist, Rafael Goldszmidt, Beatriz Kira, Anna Petherick, Toby Phillips, Samuel Webster, Emily Cameron-Blake, Laura Hallas, Saptarshi Majumdar, et al. A global panel database of pandemic policies (oxford covid-19 government response tracker). *Nature human behaviour*, 5(4):529–538, 2021.
- [17] Haidong Wang, Katherine R Paulson, Spencer A Pease, Stefanie Watson, Haley Comfort, Peng Zheng, Aleksandr Y Aravkin, Catherine Bisignano, Ryan M Barber, Tahiya Alam, et al. Estimating excess mortality due to the covid-19 pandemic: a systematic analysis of covid-19-related mortality, 2020–21. *The Lancet*, 399(10334):1513–1536, 2022.

- [18] Megan O'Driscoll, Gabriel Ribeiro Dos Santos, Lin Wang, Derek A. T. Cummings, Andrew S. Azman, Juliette Paireau, Arnaud Fontanet, Simon Cauchemez, and Henrik Salje. Age-specific mortality and immunity patterns of SARS-CoV-2. *Nature*, 590(7844):140–145, 2021.
- [19] Ryohei Mogi and Jeroen Spijker. The influence of social and economic ties to the spread of covid-19 in europe. *Journal of Population Research*, 39(4):495–511, 2022.
- [20] Yildirim Gokmen, Cigdem Baskici, and Yavuz Ercil. The impact of national culture on the increase of covid-19: A cross-country analysis of european countries. *International Journal of Intercultural Relations*, 81:1–8, 2021.
- [21] Vincenzo Alfano. Unlocking the importance of perceived governance: The impact on covid-19 in nuts-2 european regions. *Social Science & Medicine*, 343:116590, 2024.
- [22] Nicolás F Fernández-Martínez, Rafael Ruiz-Montero, Diana Gómez-Barroso, Alejandro Rodríguez-Torronteras, Nicola Lorusso, Inmaculada Salcedo-Leal, and Luis Sordo. Socioeconomic differences in covid-19 infection, hospitalisation and mortality in urban areas in a region in the south of europe. *BMC Public Health*, 22(1):2316, 2022.
- [23] Hannah Ritchie, Edouard Mathieu, Lucas Rodés-Guirao, Cameron Appel, Charlie Giattino, Esteban Ortiz-Ospina, Joe Hasell, Bobbie Macdonald, Diana Beltekian, and Max Roser. Coronavirus pandemic (covid-19). *Our World in Data*, 2021. <https://ourworldindata.org/coronavirus>.
- [24] Eurostat. Distribution of households by household size, 2022. Retrieved June, 22 2022.
- [25] N Brazeau, Robert Verity, Sara Jenks, Han Fu, Charles Whittaker, Peter Winskill, Ilaria Dorigatti, Patrick Walker, Steven Riley, Ricardo P Schnakenberg, et al. Report 34: Covid-19 infection fatality ratio: estimates from seroprevalence. 2020.
- [26] Nicholas F Brazeau, Robert Verity, Sara Jenks, Han Fu, Charles Whittaker, Peter Winskill, Ilaria Dorigatti, Patrick GT Walker, Steven Riley, Ricardo P Schnakenberg, et al. Estimating the covid-19 infection fatality ratio accounting for seroreversion using statistical modelling. *Communications medicine*, 2(1):54, 2022.
- [27] How many single-parent households are there in the eu? - products | eurostat news, 2021.
- [28] Eurostat. People in the eu: Who are we and how do we live?, 2015. Retrieved January 15, 2025.
- [29] Eurostat European Commission. The 2021 population and housing censuses in the eu, 2021. Retrieved January 15, 2025.
- [30] Frank J Elgar, Anna Stefaniak, and Michael JA Wohl. The trouble with trust: Time-series analysis of social capital, income inequality, and covid-19 deaths in 84 countries. *Social science & medicine*, 263:113365, 2020.
- [31] Dorothee Bohle and Edgars Eihmanis. East central europe in the covid-19 crisis. *East European Politics*, 38(4):491–506, 2022.
- [32] Zachary J Madewell, Yang Yang, Ira M Longini, M Elizabeth Halloran, and Natalie E Dean. Household transmission of sars-cov-2: a systematic review and meta-analysis. *JAMA network open*, 3(12):e2031756–e2031756, 2020.
- [33] Zachary J Madewell, Yang Yang, Ira M Longini, M Elizabeth Halloran, and Natalie E Dean. Factors associated with household transmission of sars-cov-2: an updated systematic review and meta-analysis. *JAMA network open*, 4(8):e2122240–e2122240, 2021.

[34] Zachary J Madewell, Yang Yang, Ira M Longini, M Elizabeth Halloran, and Natalie E Dean. Household secondary attack rates of sars-cov-2 by variant and vaccination status: an updated systematic review and meta-analysis. *JAMA network open*, 5(4):e229317–e229317, 2022.

[35] Rahul K Arora, Abel Joseph, Jordan Van Wyk, Simona Rocco, Austin Atmaja, Ewan May, Tingting Yan, Niklas Bobrovitz, Jonathan Chevrier, Matthew P Cheng, et al. Serotracker: a global sars-cov-2 seroprevalence dashboard. *The Lancet Infectious Diseases*, 21(4):e75–e76, 2021.

[36] William Msemburi, Ariel Karlinsky, Victoria Knutson, Serge Aleshin-Guendel, Somnath Chatterji, and Jon Wakefield. The who estimates of excess mortality associated with the covid-19 pandemic. *Nature*, 613(7942):130–137, 2023.

[37] Peter Bager, Jens Nielsen, Samir Bhatt, Lise Birk Nielsen, Tyra Grove Krause, and Lasse Skaftte Vestergaard. Conflicting covid-19 excess mortality estimates. *The Lancet*, 401(10375):432–433, 2023.

[38] Matshidiso Moeti, Lindiwe Makubalo, Abdou Salam Gueye, Thierno Balde, Humphrey Karamagi, Gordon Awandare, SM Thumbi, Feifei Zhang, Francisca Mutapi, and Mark Woolhouse. Conflicting covid-19 excess mortality estimates. *The Lancet*, 401(10375):431, 2023.

[39] Desmond O'Neill. Conflicting covid-19 excess mortality estimates. *The Lancet*, 401(10375):431, 2023.

[40] Jonas Schöley, Ariel Karlinsky, Dmitry Kobak, and Charles Tallack. Conflicting covid-19 excess mortality estimates. *The Lancet*, 401(10375):431, 2023.

[41] Lorenzo Pellis, Frank Ball, and Pieter Trapman. Reproduction numbers for epidemic models with households and other social structures. i. definition and calculation of r_0 . *Mathematical Biosciences*, 235(1):85–97, 2012.

[42] Béla Bollobás, Svante Janson, and Oliver Riordan. The phase transition in inhomogeneous random graphs. *Random Structures & Algorithms*, 31(1):3–122, 2007.

[43] Junyu Cao and Mariana Olvera-Cravioto. Connectivity of a general class of inhomogeneous random digraphs. *Random Structures & Algorithms*, 56(3):722–774, 2020.

[44] Kunihiro Baba, Ritei Shibata, and Masaaki Sibuya. Partial correlation and conditional correlation as measures of conditional independence. *Australian & New Zealand Journal of Statistics*, 46(4):657–664, 2004.

[45] Andrew T Levin, William P. Hanage, Nana Owusu-Boaitey, Kensington B. Cochran, Seamus P. Walsh, and Gideon Meyerowitz-Katz. Assessing the age specificity of infection fatality rates for COVID-19: systematic review, meta-analysis, and public policy implications. *European Journal of Epidemiology*, 2020.

[46] M. Bradbury, M. N. Peterson, and J. Liu. Long-term dynamics of household size and their environmental implications. *Population and Environment*, 36:73–84, 2014.

[47] A. Esteve, M. Pohl, F. Becca, et al. A global perspective on household size and composition, 1970–2020. *Genus*, 80(2), 2024.

[48] International Union for the Scientific Study of Population (IUSSP). Annual activities and management report, 2023. Retrieved January 15, 2025.

[49] Frédéric Le Play. *Les ouvriers européens*. 1877.

[50] J. Hajnal. European marriage patterns in perspective. In D. V. Glass and D. E. C. Eversley, editors, *Population in history: Essays in historical demography*, pages 101–143. Aldine Publishing Company, London and Chicago, 1965.

- [51] Peter Laslett. Family and household as work group and kin group: Areas of traditional europe compared. In R. Wall, J. Robin, and P. Laslett, editors, *Family Forms in Historic Europe*, pages 513–564. Cambridge University Press, 1983.
- [52] J. Hajnal. Two kinds of preindustrial household formation system. *Population and Development Review*, 8(3):449–494, 1982.
- [53] M. Kalmijn. Explaining cross-national differences in marriage, cohabitation, and divorce in europe, 1990-2000. *Population Studies*, 61(3):243–263, 2007.
- [54] C. Saraceno. Patterns of family living in the enlarged eu. In J. Alber, T. Fahey, and C. Saraceno, editors, *Handbook of Quality of Life in the Enlarged European Union*, pages 47–72. Routledge, London and New York, 2008.
- [55] D. S. Reher. Family ties in western europe: Persistent contrasts. *Population and Development Review*, 24(2):203–234, 1998.
- [56] M. Iacovou. Patterns of family living. In M. Iacovou and R. Berthoud, editors, *Social Europe: Living Standards and Welfare States*, pages 21–44. Edward Elgar Publishing, 2004.
- [57] Mikołaj Szołtysek. Spatial construction of european family and household systems: a promising path or a blind alley? an eastern european perspective. *Continuity and Change*, 27(1):11–52, 2012.
- [58] M. Iacovou and A. J. Skew. Household composition across the new europe: Where do the new member states fit in? *Demographic Research*, 25(14):465–490, 2011.
- [59] Anthony Giddens. *The Consequences of Modernity*. Stanford University Press, 1990.
- [60] A. W. van den Ban. Family structure and modernization. *Journal of Marriage and Family*, 29(4):771–773, 1967.
- [61] Organisation for Economic Co-operation and Development (OECD). Gross disposable income per capita of households and npish. OECD Data, 2020.
- [62] Eurostat. Living conditions in Europe - housing, 2022. Accessed January 17, 2025.
- [63] Eurofound. *Household composition and well-being*. Publications Office of the European Union, 2019.
- [64] H. Dubois and S. Nivkoski. Unaffordable and inadequate housing in europe, 2023.
- [65] L-P Béland, A Brodeur, and T Wright. The short-term economic consequences of covid-19: Exposure to disease, remote work and government response. *PLoS ONE*, 18(3):e0270341, 2023.
- [66] M Fadel, F Gilbert, C Legeay, et al. Occupational exposure to covid-19: A systematic review of the literature. *Occupational and Environmental Medicine*, 79:782–789, 2022.
- [67] E Brynjolfsson. Covid-19 and remote work: An early look at us data. 2020.
- [68] A Schmid, D Anker, J Dubois, I Bureau-Franz, N Piccardi, S Colombo Mottaz, and P Y Rodondi. Sars-cov-2 infection among employees working from home and on site: An occupational study in switzerland. *Frontiers in Public Health*, 10:980482, 2022.
- [69] Ronald Inglehart and Wayne E. Baker. Modernization, cultural change, and the persistence of traditional values. *American Sociological Review*, 65(1):19–51, 2000.
- [70] Shalom H. Schwartz. National culture as value orientations: Consequences of value differences and cultural distance. In Victor A. Ginsburgh and David Throsby, editors, *Handbook of the Economics of Art and Culture*, volume 2, pages 547–586. Elsevier, 2014. See p. 558 for detailed discussion.

- [71] Shalom H. Schwartz. A theory of cultural value orientations: Explication and applications. *Comparative Sociology*, 5(2–3):137–182, 2006.
- [72] Andreas Käffer and Jörg Mahlich. Culture and covid-19-related mortality: a cross-sectional study of 50 countries. *Journal of Public Health Policy*, 43:413–430, 2022.
- [73] Alexander Ibanez and Gaurav S. Sisodia. The role of culture on 2020 sars-cov-2 country deaths: a pandemic management based on cultural dimensions. *GeoJournal*, 87(2):1175–1191, 2022.
- [74] Chia-Ying Chen, Carl Benedikt Frey, and Giorgio Presidente. Culture and contagion: Individualism and compliance with covid-19 policy. *Journal of Economic Behavior & Organization*, 190:191–200, 2021.
- [75] Yining Chen and Md Iqbal Biswas. Impact of national culture on the severity of the covid-19 pandemic. *Current Psychology*, 42:15813–15826, 2023.
- [76] M. J. Gelfand, J. C. Jackson, X. Pan, D. Nau, D. Pieper, E. Denison, and M. Wang. The relationship between cultural tightness–looseness and covid-19 cases and deaths: a global analysis. *The Lancet Planetary Health*, 5(3):e135–e144, 2021.
- [77] T. J. Bollyky, E. N. Hulland, R. M. Barber, J. K. Collins, S. Kiernan, M. Moses, and J. L. Dieleman. Pandemic preparedness and covid-19: an exploratory analysis of infection and fatality rates, and contextual factors associated with preparedness in 177 countries, from jan1,2020 to sept30,2021. *The Lancet*, 399(10334):1489–1512, 2022.
- [78] Eurostat. Young people - housing conditions, 2023. Statistics Explained.

Supplementary Material

The Supplementary Material provides an in-depth overview of our research methodology, including detailed analysis methods and data sources. It includes a sensitivity analysis that assesses the robustness of our results to modeling assumptions, data source uncertainties, and key parameters. Additionally, an expanded sociological analysis of our findings is presented, along with supplementary figures and tables that display the data referenced in the manuscript and define relevant variables and parameters.

Contents

S1 Extended methods	21
S1.1 Prevalence estimation	21
S1.1.1 Estimation of country-specific infection fatality rates (CIFRs)	21
S1.1.2 Estimation of γ -extended COVID-19 deaths	22
S1.1.3 Estimation of γ	23
S1.1.4 Comparison of excess mortality estimates and γ -extended COVID-19 deaths	25
S2 Social determinants of household size	25
S2.1 Economic factors	26
S2.2 Cultural factors	27
S2.3 Institutional factors	28
S3 Robustness check	29
S4 Supplementary Tables	30
S5 Supplementary Figures	30

S1 Extended methods

S1.1 Prevalence estimation

Estimating the prevalence α is a challenging task. For example, reporting practices and capabilities vary widely across countries, leading the number of officially reported COVID-19 cases to deviate substantially from the true number of cases. A more reliable method for obtaining a prevalence estimate involves using death reports and country-specific infection fatality rates (CIFRs). Given a death and a CIFR estimate, the prevalence α can be estimated by

$$\alpha = \frac{D}{\text{CIFR}}, \quad (1)$$

where D is the number of deaths. Our approach to estimating the true prevalence consists of two steps. First, we estimate the CIFRs based on [25, 26]. Second, we estimate the true number of COVID-19 deaths using observed surplus and reported COVID-19-related deaths. We cover the period from the start of the pandemic until June 13th, 2021. We chose this end date for two reasons. First, it is early enough that mass vaccinations have not yet had a significant effect on reducing COVID-19-related deaths. Second, it represents a date at which infection numbers were low across all European countries [23].

S1.1.1 Estimation of country-specific infection fatality rates (CIFRs)

Age is one of the dominant factors for COVID-19 severity and fatality risk [18, 26, 45]. The marked exponential dependency of COVID-19 infection fatality rate (IFR) on age has some noise in the extremes of the very young and very old. We used the age-dependent IFR and confidence intervals reported in [26] to reconstruct the uncertainty curve, i.e., estimate the parameters of the uncertainty log-normal distribution around each age point.

Let $s = 1, \dots, N$ be the age groups used for reporting the age-dependent IFR^s and A^s the collection of discrete ages encompassed in age group s . For example, if age group k represents the age range $[a_1^k, a_2^k]$, then $A^k = \{a_1^k, a_1^k + 1, \dots, a_2^k - 1, a_2^k\}$. Let further

$$\xi^* = \underset{\xi}{\operatorname{argmin}} \sum_{s=1}^N \left(\frac{\text{IFR}^s \sum_{i \in A^s} p_i - \sum_{i \in A^s} p_i f_{\text{IFR}}(i; \xi)}{\sum_{i \in A^s} p_i} \right)^2 \quad (2)$$

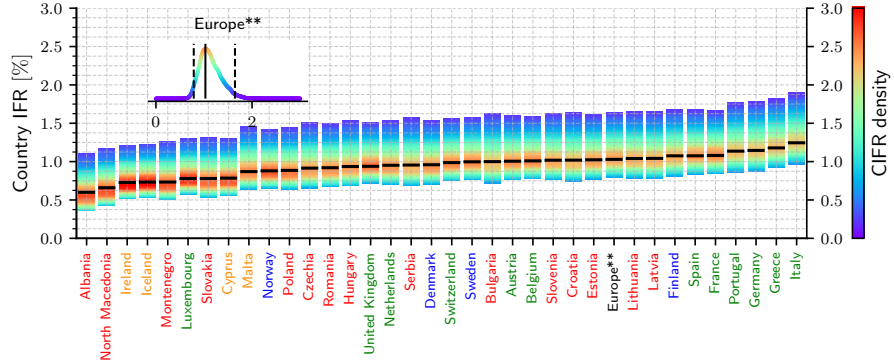
where $\xi = [\alpha \ \beta \ \gamma \ \delta]$ and

$$f_{\text{IFR}}(i; \xi) = e^{\alpha h(i; \xi) + \beta} \quad (3)$$

$$h(i; \xi) = \frac{i}{2} - \frac{1}{2\gamma} \log \left(\frac{\cosh[\gamma(i - \delta)]}{\cosh[\gamma(-\delta)]} \right). \quad (4)$$

These functions were selected to capture the exponential dependency of IFR on age, with saturation for high ages (above 90 years). In this context, Eq. 4 represents the saturation component of the exponent in Eq. 3. For a given sample mortality curve parameter vector (ξ) (i.e., the result of reconstructing the mortality curve (f_{IFR}) from the uncertainty distributions at each point), we can estimate the country-specific IFR (scalar) as a weighted average using the above formula as follows

$$\text{CIFR} = \sum_{i=0}^M p_i f_{\text{IFR}}(i; \xi), \quad (5)$$



Supplementary Figure S1: **Country infection fatality rate (CIFR) estimation for different countries.** We compute country-specific IFRs using age-resolved estimates of the IFR [25, 26] and country demographics. Given that age-resolved IFRs are reported as a distribution, we draw 50,000 samples and fit an exponential function to capture the correlation between measurements. We use the fitted profile as an estimated CIFR and weight it by country demographics to obtain a country-specific IFR (color scheme). The vertical bars extend until the 10th and 90th percentiles, and the black bar indicates the median. Europe marked with a double asterisk (**) includes only countries for which we have full Eurostat data.

where p_i is a fraction of the population at age i in a given country and M is the maximum age in the population. Note that the mortality curve is the same for all countries (for the same params vector ξ) and that the differences in CIFRs between countries are due to the population's age profile (demographics).

S1.1.2 Estimation of γ -extended COVID-19 deaths

Determining the true number of COVID-19-related deaths D is challenging, e.g., because many COVID-19 reported deaths were not officially counted as such. To find an accurate estimate, we thus add the officially reported COVID-19 deaths to the maximum number of weekly deaths over previous years — if we observed even more deaths than that, we attribute a fraction γ of those to being COVID-19 related (Fig. S2). We call this estimate the γ -extended number of COVID-19 deaths. Similar adjustments are sometimes also known as *excess deaths* [23].

In particular, we use the following procedure.

1. We normalize deaths $D_a(T)$ in the year J using population size $P_a(J)$

$$d_a(T) := D_a(T) / P_a(J).$$

2. We find the maximum number of deaths in each week w over previous years

$$d_a^{\max}(w) := \max_{J \in [2015, 2019]} \{d_a(T)\}.$$

3. Using a three-week moving average, we smoothen the maximum deaths

$$d_a^*(w) := \frac{1}{3} (d_a^{\max}(w-1) + d_a^{\max}(w) + d_a^{\max}(w+1)).$$

4. We calculate surplus deaths $S_a(T)$ as

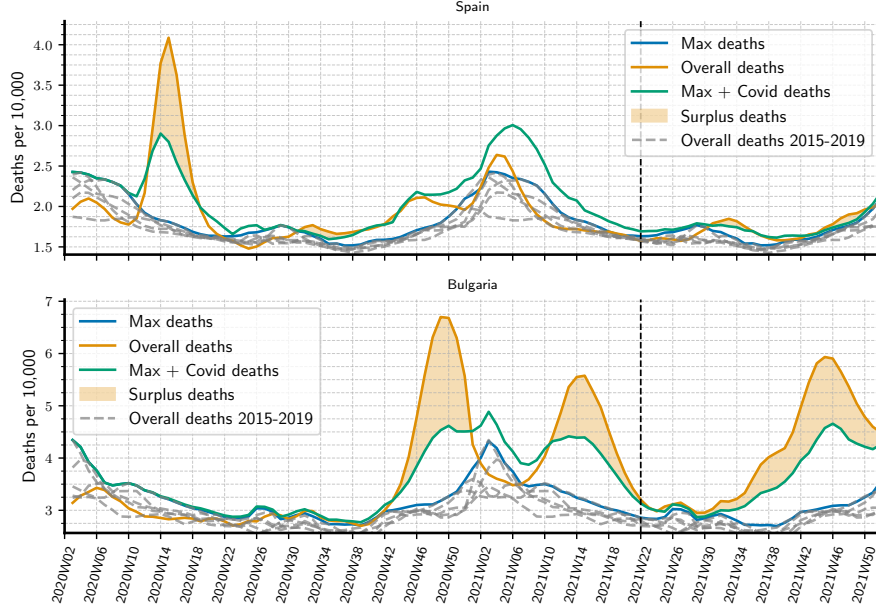
$$S_a(T) := \max \{0, P_a(J) \cdot \max \{d_a(T) - d_a^*(w), 0\} - C_a(T)\}$$

5. For a specific value of γ , we calculate γ -extended COVID-19 deaths $E_a(T, \gamma)$:

$$E_a(T, \gamma) := C_a(T) + \gamma \cdot S_a(T).$$

This procedure is visually represented in Fig. S2. Compared to the officially reported COVID-19 deaths, this method substantially increases the death estimate in some countries (Fig. S3).

Combined with the IFR estimates, we thus obtain a distribution over prevalences (Fig. S4).



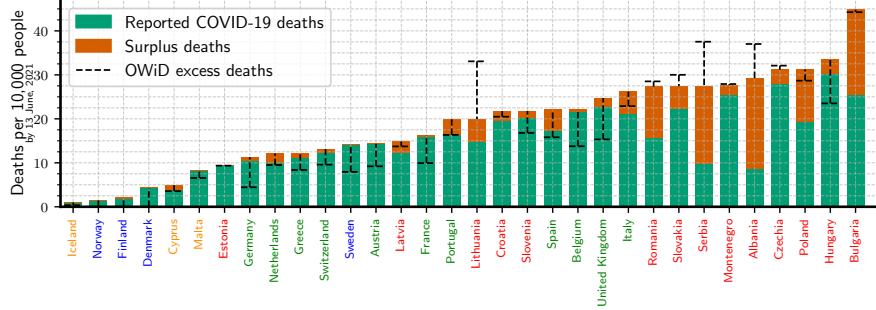
Supplementary Figure S2: **Example estimation of total COVID-19 deaths for Bulgaria and Spain.** The blue curve shows the maximal weekly deaths over 2015–2019. It is added to the officially reported COVID-19 deaths (green curve). If the overall deaths in any given week during the pandemic exceed this green curve (orange shaded area), we attribute a fraction γ of these additional deaths as being COVID-19 related. This way, we obtain the γ -extended COVID-19 death estimate. The dashed line represents the end date of our γ -extended deaths and prevalence estimations.

S1.1.3 Estimation of γ

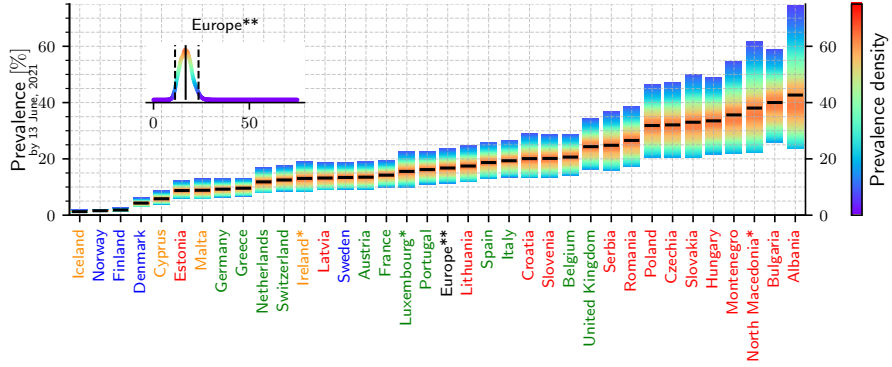
One of the central parameters in our analysis is γ , i.e., the fraction of the surplus deaths attributable to COVID-19. However, this parameter is hard to estimate. Analyses of the availability and delivery of healthcare services during the pandemic support the hypothesis that excess mortality during the pandemic was mainly attributed to COVID-19-related infections.

Overall, excess mortality coincided with successive waves of infection, during which healthcare systems operated under unusual conditions. Mortality during these periods may have been related to direct SARS-CoV-2 infections or indirect effects related to healthcare access and delivery. To assess this, we analyzed data from the Polish National Health Fund on urgent medical interventions, including procedures such as treatment of stroke, heart attack, and aneurysm perforation. These services, if left untreated, usually lead to mortality within timescales comparable to waves of infection.

We use the following procedure to estimate the fraction γ of additional deaths that we attribute to being COVID-19 related.



Supplementary Figure S3: The officially reported number of COVID-19 deaths, surplus deaths, and γ -Extended deaths, estimated as described in the main text. Cumulative officially reported COVID-19 deaths are represented by green bars, and cumulative excess deaths are represented by orange bars. The sum of these bars corresponds to the number of γ -extended COVID-19 deaths where γ equals 1. For countries marked with an asterisk (*), the excess of deaths is 0 due to incomplete Eurostat data. Europe marked with a double asterisk (**) uses aggregated data from countries without an asterisk (all data were available).



Supplementary Figure S4: **Prevalence estimation for different countries.** We obtain a distribution over the prevalence by Using the estimated COVID-19 deaths and the country infection fatality rate (CIFR) estimates. Vertical bars extend to the 10th and 90th percentiles, and the black bar indicates the median. For countries marked with an asterisk (*), the excess of deaths is 0 due to incomplete Eurostat data. Europe, marked with a double asterisk (**), uses aggregated data from countries without an asterisk (all data were available).

1. We find the mean number of emergency interventions in each week w over previous years and smooth them

$$BL(w) = \frac{1}{5} \sum_{j=2015}^{2019} \frac{1}{3} (EI(w-1, j) + EI(w, j) + EI(w+1, j))$$

2. We calculate the lacking procedures during the weeks of the pandemic

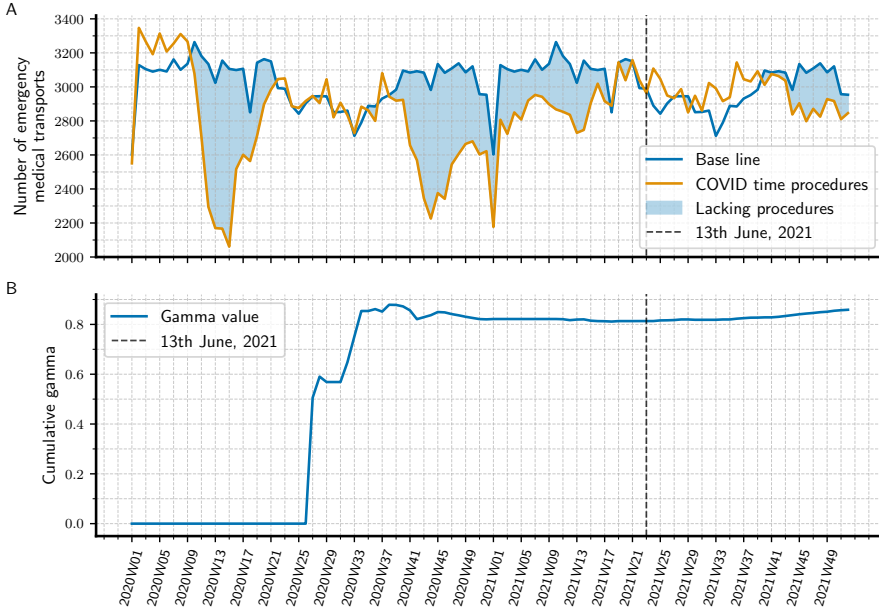
$$LP(w, J) = \max\{0, BL(w) - EI(w, J)\}$$

3. We estimate the parameter γ using the surplus deaths $S(w)$

$$\gamma(w, J) = \frac{\sum_{j=2020}^J \sum_w^{N_j} \max\{0, S(w) - LP(w, j)\}}{\sum_{j=2020}^J \sum_w^{N_j} S(w)}$$

where $N_j = w$ if $j = J$ and $N_j = 52$ if $j < J$.

Fig. S5 shows a visual representation of this procedure. We estimate γ to lie in the range of $\gamma \approx 0.85$, which we used in the analysis in the main text.



Supplementary Figure S5: **A.** Number of emergency procedures due to all causes except COVID-19 in Poland, before and during the pandemic. **B.** Cumulative deviation from historical trends, which is a proxy for γ .

S1.1.4 Comparison of excess mortality estimates and γ -extended COVID-19 deaths

Estimates of excess mortality from Our World in Data are calculated using a linear model [14]. The model is based on linear regression fitted to historical weekly mortality data from 2015-2019, which provides a baseline for expected deaths in subsequent years. Excess mortality is the cumulative difference between observed deaths in a given week and the model's predicted baseline for that week. This approach allows negative excess mortality in some weeks, which often yields lower excess mortality estimates than our method. In addition, the model does not include officially reported COVID-19 deaths in its estimates, which can result in even lower COVID-19 excess mortality estimates, particularly at the beginning of the pandemic.

S2 Social determinants of household size

The COVID-19 pandemic has highlighted the social context's essential role in shaping responses to health crises, particularly that of households. As fundamental social units, households influence not only the transmission of infections but also the beliefs, behaviors, and coping strategies that guide individual responses to health emergencies. This study positions the household as the primary unit of analysis, recognizing that its diversity in size and structure is critical for understanding the dynamics of infection spread.

As illustrated in Fig. S8, the effective household size η^* (i.e., mean household size plus a –positive– variance-dependent correction factor) correlates with the out-household reproduction number \bar{R}_{out} values. To understand how household size affects \bar{R}_{out} and may shape pandemic-response patterns, we must view household structures as outcomes of long-run economic and cultural processes. A global trend toward smaller households has been evident for centuries, particularly in developed countries [46]. This trend is particularly

pronounced in Europe, though significant regional variation in household composition remains [47, 48] (Esteve et al., 2023; N-IUSSP, 2023). Household structure across Europe can be categorized into four broad regions: Western, Eastern, Southern, and Nordic Europe. This distinction, first conceptualized by Frédéric Le Play in the 1870s and later popularized by John Hajnal in the 1960s, reflects enduring patterns of family composition [49, 50]. Studies support this categorization, with Nordic countries exhibiting a high prevalence of single-person households, Western Europe dominated by nuclear families, Southern Europe characterized by larger family units, and Eastern Europe showing extended family systems [51–58].

There is a strong correlation between household size and the HDI (Fig. 4A), particularly with the economic component (GNI). These West/North-East/South differences in household size can be analyzed using modernization theory. This theory posits that as societies undergo economic development, they experience structural and cultural changes that transform social institutions, including family structures, which directly affect household size (urbanization, industrialization, income growth, mobility) [59, 60]. Economic growth, a core element of modernization, promotes the emergence of more independent family units, leading to smaller households. As traditional values give way to individualistic cultural frameworks, societies shift from multigenerational households to nuclear families or single-person households [47, 58]. While HDI does not directly measure cultural patterns, it indirectly reflects cultural transformations driven by shifts in the economy and society. For example, the expansion of women's education increases their income potential, promotes financial independence, shapes career aspirations, often leads to lower fertility rates, and ultimately changes the accepted family model.

The size and structure of households are shaped by a combination of economic, cultural, and institutional factors. These same factors not only determine household size but also affect how societies respond to pandemics. For instance, factors like housing conditions, employment structures, and welfare support systems influence both household size and the ability to implement health measures such as isolation and social distancing. By analyzing the determinants of household size, we also gain insight into the broader mechanisms that shape pandemic risk and public health outcomes. These factors will be briefly discussed.

S2.1 Economic factors

Economic conditions, particularly income levels and housing costs, shape household size across Europe. Wealthier regions like Western and Northern Europe exhibit smaller households, often nuclear families or single-person units, driven by financial independence and strong social safety nets. Countries such as Switzerland and Luxembourg, which report the highest GNI and disposable incomes, illustrate this trend. Even in Northern Europe, where welfare systems reduce disposable income (e.g., Norway: \$32,514; Denmark: \$25,859), household sizes remain small due to comprehensive welfare systems. In contrast, Southern and Eastern Europe face greater economic challenges, such as lower GNI and higher unemployment, housing cost and poor welfare system leading to larger household sizes. Families in countries like Italy (GNI: \$39,294) and Greece (GNI: \$21,391) often rely on shared resources and multigenerational living due to limited financial independence. This pattern is most prominent in Eastern Europe, where lower disposable incomes, as seen in Romania (\$12,635) and Bulgaria (\$12,092), drive families toward shared living arrangements. Data reported in [61, 62]. Better housing conditions reduce overcrowding in wealthier countries like the Netherlands and Belgium. By contrast, overcrowding rates exceeding in Bulgaria, Latvia, Romania, and Poland (over 1/3 people living in an overcrowded household) result in higher household density, driven by inadequate housing and economic insecurity [29, 63, 64], which may elevate infection risk during pandemics.

Modernization theory explains how differences in economic development between Western/Northern and Eastern/Southern Europe shape employment structures. Consequently, varying levels of economic growth are expected to result in differences in occupational structure and work organization, which can play a crucial role in pandemic control, i.e., the share of the labor force working in the industry, services where there is frequent social contact and professionals with less social contact and possible remote work. For instance, higher economic development in Western and Northern Europe facilitates greater use of remote work and flexible work arrangements, reducing physical proximity and the risk of infection. Remote work rates in 2020 were highest in Finland (24.82%), Luxembourg (23.01%), and Ireland (21.13%). In contrast, remote work was less common in Southern and Eastern Europe, with Latvia (2.87%), Romania (3.18%), and Croatia (3.48%) reporting the lowest rates. In regions with lower economic development, like Eastern and Southern Europe, employment is often concentrated in site-specific sectors such as manufacturing, construction, and mining, where on-site presence is essential, increasing exposure to infection risks. Occupations requiring physical presence faced higher risks of infection and suffered more significant economic consequences. In contrast, those able to work from home were better protected both health-wise and economically, underscoring the importance of remote work capabilities in mitigating the effects of public health crises [65–68].

S2.2 Cultural factors

Cultural factors reinforce the East-South versus West-North divide in household size. Culture values such as embeddedness, collectivism, more pronounced in the East and South, contribute to larger, multigenerational households, while autonomy & individualist values in the West and North support smaller, nuclear, or single-person households [69, 70].

There is a reciprocal relationship between culture and household size: cultural values shape family size, and the model of family size reinforces certain cultural orientations. The size of a country's average family or household strongly correlates with cultural values, where larger households emphasize embeddedness, hierarchy, and mastery. These cultural orientations arise from societal norms that prioritize obedience, conformity, and collective interest to maintain order and effective coordination within large family structures. In turn, these norms foster cultural frameworks that support tradition, authority, and group cohesion, making autonomy and egalitarianism less compatible with such settings [71].

Culture also affects the strength of family ties, which is reflected in frequency of social contacts. For example, young adults in Southern and Eastern Europe often remain in the parental home for longer periods due to stronger social ties. By contrast, young adults in Western and Northern Europe leave home earlier, influenced by cultural norms promoting early independence and institutional support systems for housing and education. Cultural patterns significantly influence societal beliefs and behaviors, affecting compliance with restrictions during the COVID-19 pandemic [20, 72–75].

For instance, Gelfand's research indicates that societies with strict social norms ("tight" cultures) experienced fewer COVID-19 cases and deaths compared to more permissive ("loose") cultures [76]. Studies suggest that low trust in governments correlates with higher infection rates [77]. In Nordic countries, there is a high level of trust, whereas in central-eastern-European countries, levels of trust in government and among individuals are markedly lower [31]. Therefore, the variation in infection rates can be partly attributed to cultural patterns influencing adherence to restrictions and the prevailing levels of trust within a society.

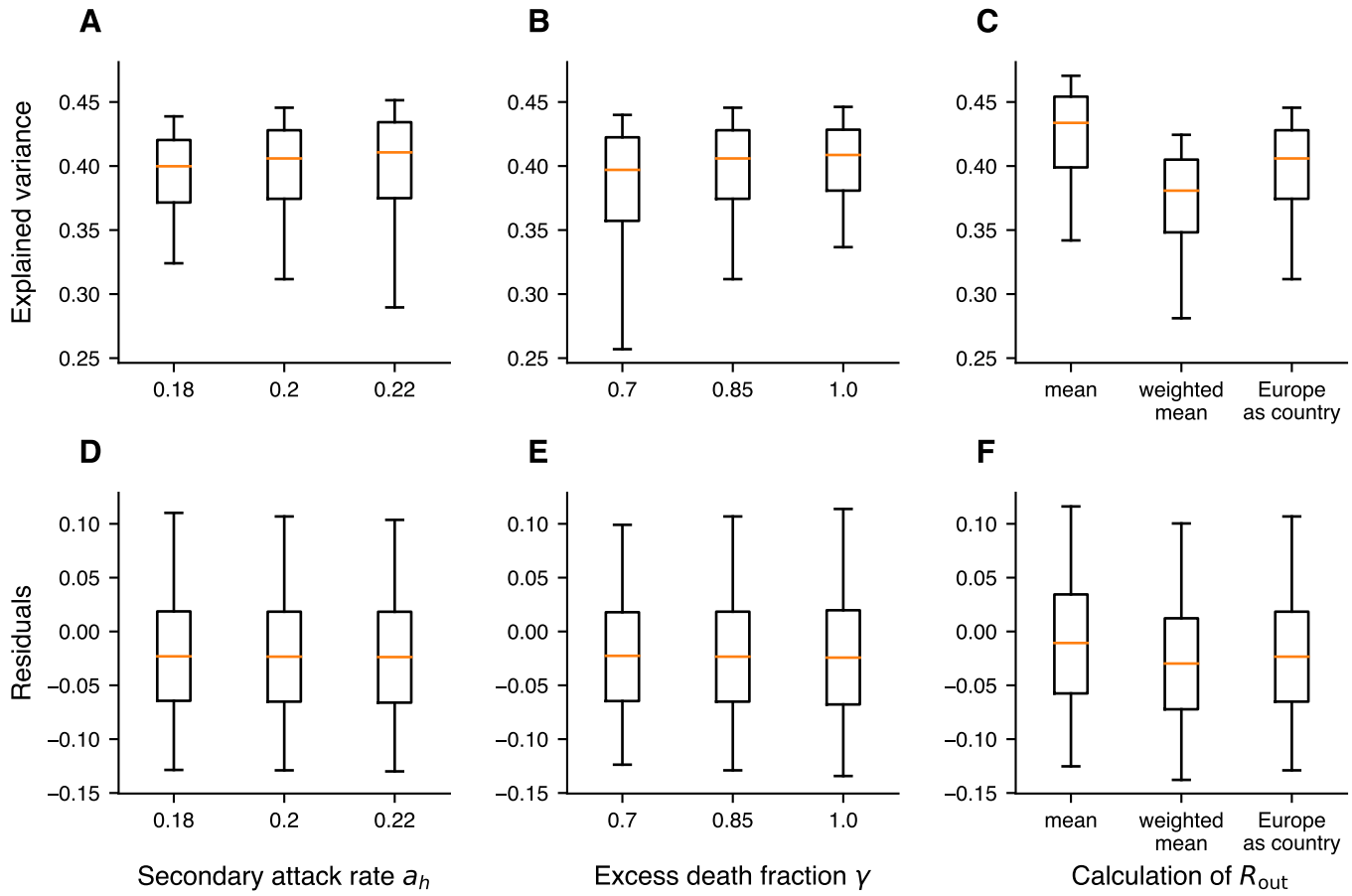
S2.3 Institutional factors

Finally, institutional factors, i.e., society's forms of organizations, shape household size and influence pandemic outcomes. The North/West vs. East/South divide is reflected in the prevalence of co-residence between older and younger family members and the availability of formalized care facilities for the elderly. When state-provided care is limited, family-based care increases, leading to higher co-residence rates within households. Welfare states in Scandinavia provide support through childcare, eldercare, and housing assistance, enabling individual independence and smaller household sizes. For instance, in Nordic countries such as Norway (highest), Denmark, Finland, and Sweden, over 12% of the 80+ population reside in formalized care facilities for older people. This rate rises to 16% in Luxembourg and Switzerland and 24% in Belgium. In contrast, Poland exhibits much lower rates, with less than 1% of the 65+ population living in formalized care facilities, increasing only slightly to 1.6% for the 80+ population (<https://nhwstat.org/>). State-funded eldercare systems reduce co-residence rates for older adults. For instance, 5% of those over 65 in Nordic countries live with younger household members (aged 50 or below), compared to 38% in Poland—the highest rate in Europe [61, 78]. Weaker welfare systems in Southern and Eastern Europe increase reliance on family support, leading to larger, multigenerational households. While eldercare systems reduce co-residence, they also increase the share of older adults living in formal care institutions. During the COVID-19 pandemic, this arrangement posed infection risks in eldercare facilities, highlighting the dual role of welfare systems in shaping household structure and pandemic outcomes.

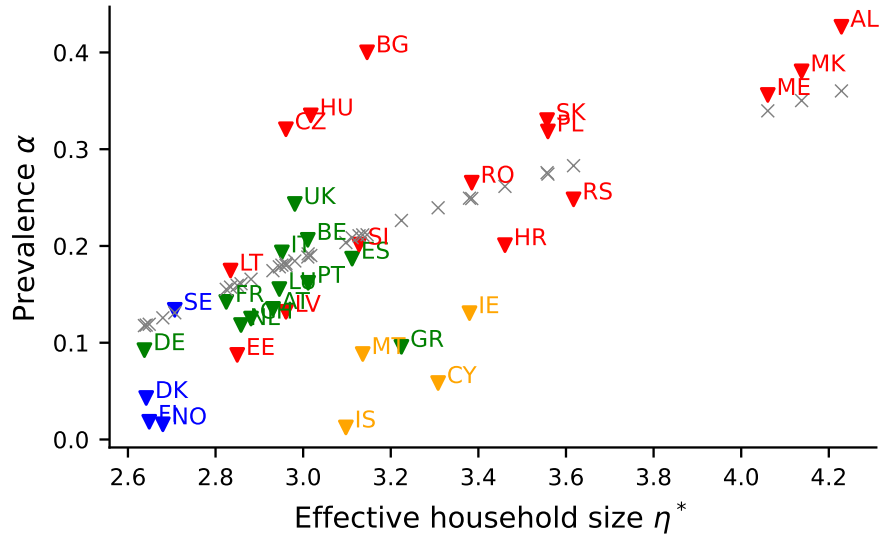
In summary, prolonged modernization processes—such as shifts in labor market structures, technological advancements, and changes in income distribution—have significantly influenced family models and household sizes. While numerous studies emphasize the impact of cultural factors, our analysis of correlations and partial correlations reveals a discernible pattern: economic and structural factors exert a more substantial influence on social contact structure. We interpret this as follows: structural factors directly shape individual behaviors by limiting opportunities for social interactions (e.g., household size or remote work), whereas cultural factors, being more nuanced, affect social networks in a complex and indirect manner.

S3 Robustness check

Given the uncertainty around the IFR and the fraction of surplus deaths that are to be attributed to COVID-19 (γ), we proceed iteratively, sampling from the IFR distribution (multivariable) to generate several IFR vectors, which will yield new estimates for the country IFR. We repeat this procedure 50 000 times and estimate a distribution for the theoretical prevalence according to equation 1. This allows us to quantify not only the out-household reproduction number (and thereby have a fair way to compare pandemic management, ruling out the effect of households), but also the uncertainty around this value. The overall methodology is summarized in Fig. 1C.



Supplementary Figure S6: **Robustness of our results before variations in assumed parameters.** Orange markers denote the median, boxes the interquartile ranges, and whiskers the 10-90 percentiles.



Supplementary Figure S7: **Relation between prevalence and effective household sizes.** Same as Fig. 2A, but with ISO-2 country codes. Theoretical prevalences (gray crosses) are computed assuming a common European out-household reproduction number $R_{\text{out},\text{Europe}}$ in all countries. $R_{\text{out},\text{Europe}}$ is computed by treating Europe as a proper country.

S4 Supplementary Tables

S5 Supplementary Figures

Table S1: **Data overview.** CIFR denotes the country-infection fatality rate, D the officially reported COVID-19 deaths, S the surplus deaths (Sec. S1.1.2), α the estimated prevalence, $\bar{\eta}$ and η^* the mean and effective household size respectively, and \bar{R}_{out} the out-household reproduction number. For countries marked with an asterisk (*), prevalence is based on officially reported COVID-19 deaths due to missing data on overall fatalities. Europe (**) uses aggregated data from countries without an asterisk. For distributions, values represent the median and values in brackets the 95% CI.

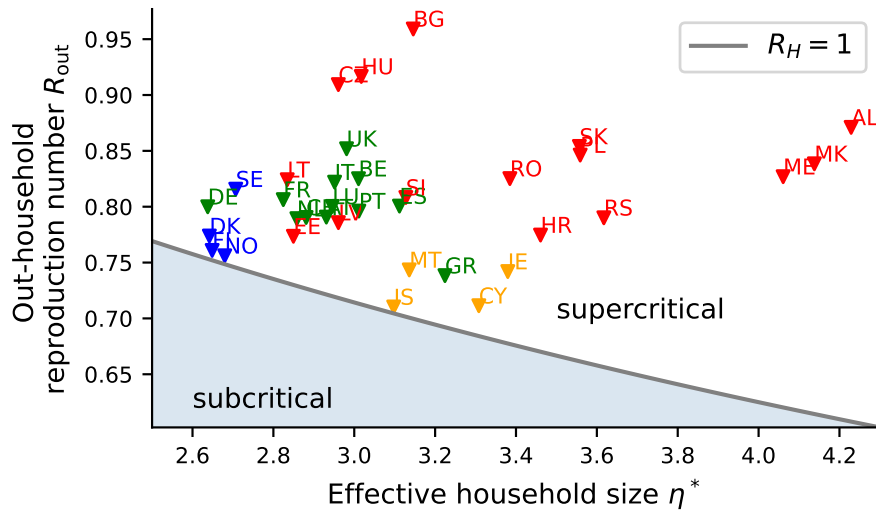
	CIFR	D	S	α	E	η^*	\bar{R}_{out}
Albania	0.60 [0.38, 1.01]	8.62	20.51	42.67 [25.70, 68.81]	3.63	4.23	0.87 [0.73, 1.36]
Austria	1.01 [0.79, 1.50]	14.27	0.07	13.50 [9.54, 18.13]	2.20	2.93	0.79 [0.77, 0.82]
Belgium	1.01 [0.81, 1.50]	21.57	0.64	20.64 [14.78, 27.41]	2.27	3.01	0.83 [0.78, 0.88]
Bulgaria	1.00 [0.75, 1.53]	25.42	19.41	40.02 [27.46, 55.74]	2.37	3.15	0.96 [0.84, 1.18]
Croatia	1.02 [0.78, 1.54]	19.55	2.22	20.09 [13.95, 27.62]	2.71	3.46	0.77 [0.73, 0.83]
Cyprus	0.78 [0.58, 1.22]	3.92	1.01	5.84 [3.91, 8.21]	2.64	3.31	0.71 [0.70, 0.73]
Czechia	0.92 [0.69, 1.41]	27.90	3.28	32.07 [21.79, 44.75]	2.34	2.96	0.91 [0.83, 1.05]
Denmark	0.96 [0.73, 1.44]	4.23	0.08	4.29 [2.98, 5.86]	1.98	2.64	0.77 [0.77, 0.78]
Estonia	1.02 [0.80, 1.52]	9.36	0.08	8.74 [6.20, 11.73]	2.11	2.85	0.77 [0.76, 0.79]
Finland	1.08 [0.84, 1.58]	1.74	0.37	1.83 [1.30, 2.46]	1.96	2.65	0.76 [0.76, 0.76]
France	1.08 [0.87, 1.56]	16.05	0.26	14.22 [10.40, 18.62]	2.14	2.82	0.81 [0.78, 0.84]
Germany	1.15 [0.91, 1.68]	10.51	0.78	9.24 [6.64, 12.30]	2.00	2.64	0.80 [0.78, 0.82]
Greece	1.18 [0.95, 1.71]	11.16	0.97	9.58 [7.00, 12.60]	2.55	3.22	0.74 [0.72, 0.76]
Hungary	0.94 [0.71, 1.44]	30.25	3.21	33.51 [22.97, 46.33]	2.30	3.02	0.92 [0.83, 1.06]
Iceland	0.73 [0.56, 1.15]	0.97	0.00	1.25 [0.84, 1.72]	2.32	3.10	0.71 [0.71, 0.71]
Ireland*	0.73 [0.54, 1.13]	9.88	0.00	13.06 [8.74, 18.21]	2.62	3.38	0.74 [0.72, 0.78]
Italy	1.25 [1.00, 1.79]	21.12	5.05	19.34 [14.19, 25.37]	2.30	2.95	0.82 [0.79, 0.87]
Latvia	1.04 [0.81, 1.55]	12.33	2.51	13.20 [9.31, 17.86]	2.24	2.96	0.79 [0.76, 0.82]
Lithuania	1.04 [0.82, 1.55]	14.86	5.09	17.46 [12.35, 23.55]	2.16	2.83	0.82 [0.79, 0.87]
Luxembourg*	0.78 [0.60, 1.22]	12.86	0.00	15.55 [10.55, 21.37]	2.28	2.95	0.80 [0.77, 0.84]
Malta	0.87 [0.67, 1.36]	8.13	0.10	8.83 [6.02, 12.27]	2.46	3.14	0.74 [0.73, 0.77]
Montenegro	0.73 [0.53, 1.17]	25.45	2.18	35.62 [23.30, 51.40]	3.26	4.06	0.83 [0.73, 1.02]
Netherlands	0.95 [0.73, 1.44]	10.01	2.12	11.83 [8.20, 16.20]	2.14	2.86	0.79 [0.77, 0.82]
North Maced.*	0.66 [0.45, 1.09]	25.92	0.00	38.06 [23.86, 57.46]	3.52	4.14	0.84 [0.72, 1.11]
Norway	0.88 [0.68, 1.33]	1.45	0.00	1.57 [1.09, 2.13]	1.97	2.68	0.76 [0.75, 0.76]
Poland	0.89 [0.67, 1.35]	19.31	11.92	31.85 [21.74, 43.94]	2.76	3.56	0.85 [0.77, 0.97]
Portugal	1.14 [0.90, 1.67]	16.40	3.49	16.20 [11.62, 21.60]	2.46	3.01	0.80 [0.77, 0.84]
Romania	0.92 [0.70, 1.40]	15.69	11.65	26.55 [18.23, 36.62]	2.57	3.38	0.83 [0.76, 0.92]
Serbia	0.96 [0.71, 1.47]	9.85	17.62	24.82 [16.90, 34.73]	2.84	3.62	0.79 [0.74, 0.88]
Slovakia	0.78 [0.56, 1.23]	22.39	5.02	33.02 [21.71, 47.26]	2.86	3.56	0.85 [0.77, 1.01]
Slovenia	1.02 [0.79, 1.53]	20.35	1.46	20.15 [14.13, 27.30]	2.44	3.13	0.81 [0.77, 0.87]
Spain	1.08 [0.87, 1.58]	17.26	4.79	18.69 [13.51, 24.65]	2.49	3.11	0.80 [0.77, 0.85]
Sweden	1.00 [0.79, 1.48]	14.16	0.00	13.40 [9.55, 17.91]	1.98	2.71	0.82 [0.79, 0.85]
Switzerland	0.99 [0.78, 1.47]	12.29	0.86	12.50 [8.84, 16.75]	2.18	2.88	0.79 [0.77, 0.82]
United Kingdom	0.94 [0.75, 1.42]	22.89	1.85	24.35 [17.22, 32.65]	2.31	2.98	0.85 [0.80, 0.93]

Table S2: **Overview of Pearson and semi-partial correlation coefficients between the estimated prevalence α and variable Y .** Z denotes the confounding variable and the relative correlation change is defined by 1 - semi-partial / Pearson and given in percent. Note that a relative correlation change of $< -100\%$ can arise if the Pearson correlation is negative but the semi-partial correlation is positive. Values in brackets denote the 95% CIs.

Variable Y	Pearson r	Partial ($Z = \eta^*$)	Rel. change ($Z = \bar{R}_{\text{out}}$)	Partial ($Z = \eta^*$)	Rel. Change ($Z = \bar{R}_{\text{out}}$)
HDI	-0.79 [-0.80, -0.77]	-0.52 [-0.69, -0.12]	-34% [-94%, -11%]	-0.72 [-0.74, -0.67]	-8% [-19%, -4%]
GNI	-0.64 [-0.66, -0.63]	-0.39 [-0.55, -0.05]	-40% [-102%, -14%]	-0.63 [-0.64, -0.60]	-2% [-11%, 2%]
Life expectancy	-0.69 [-0.69, -0.68]	-0.56 [-0.65, -0.28]	-19% [-67%, -35%]	-0.48 [-0.50, -0.45]	-30% [-36%, -27%]
Years of schooling	-0.37 [-0.37, -0.37]	-0.16 [-0.27, 0.06]	-57% [-126%, -24%]	-0.46 [-0.46, -0.45]	+25% [21%, 26%]

Table S3: **Statistical significance of results in Tab. S2.** Values and brackets denote the median and 95% CI for the p value distribution associated to the different correlations.

Variable Y	p (Pearson r)	p (Partial, $Z = \eta^*$)	p (Partial $Z = \bar{R}_{\text{out}}$)
HDI	2.15×10^{-8} [2.15×10^{-8} , 2.15×10^{-8}]	1.51×10^{-3} [1.70×10^{-6} , 0.69]	1.09×10^{-6} [4.18×10^{-7} , 2.30×10^{-5}]
GNI	2.90×10^{-5} [1.85×10^{-5} , 4.57×10^{-5}]	0.021 [0.41×10^{-3} , 0.83]	4.18×10^{-5} [2.82×10^{-5} , 0.26×10^{-3}]
Life expectancy	5.61×10^{-6} [5.33×10^{-6} , 7.52×10^{-6}]	0.49×10^{-3} [1.72×10^{-5} , 0.20]	0.0034 [0.0022, 0.0086]
Years of schooling	0.030 [0.029, 0.030]	0.36 [0.10, 0.95]	0.0054 [0.0053, 0.0074]



Supplementary Figure S8: **Critical out-household reproduction number** $R_{\text{out}}^{\text{crit}} = \mathcal{B}^{-1}$. The effective household size η^* defines a critical out-household reproduction number that, if exceeded, leads to a household reproduction number $\mathcal{R}_H > 1$. Countries with a high effective household size η^* have to reduce the out-household reproduction number substantially lower to contain an outbreak than countries with a low η^* . Note that all countries lie in the supercritical region, as they all experienced COVID-19 outbreaks.